

Temporal CSI Correlation in Mixed RF/FSO Cooperative Relaying Systems Under Joint Effects of HPA Nonlinearities and IQ Imbalance

Elyes Balti, *Member, IEEE*, Neji Mensi, *Member, IEEE*, and Danda B. Rawat, *Senior Member, IEEE*

Abstract—In this paper, we present the performance analysis of mixed RF/FSO system with multiple relays. To select the best relay, we adopt partial relay selection with outdated CSI wherein we investigate the effect of the temporal correlation of the channels. Unlike the vast majority of work, we introduce the impairments to the relays and the destination and we compare the performance against conventional RF relaying systems. We further derive the expressions of the outage probability and the ergodic capacity as well as the bounds to unpack engineering insights into the system robustness.

Index Terms—Soft Envelope Limiter, Traveling Wave Tube Amplifier, IQ Imbalance, Amplify-and-Forward, Partial Relay Selection, Outdated CSI.

I. INTRODUCTION

Wireless optical communications also known as Free-Space Optic (FSO) is considered as the key stone for the next generation of wireless communication since it has recently gained enormous attention for the vast majority of the most well-known networking applications such as fiber backup, disaster recoveries and redundant links [1]. The main advantages of employing the FSO is to reduce the power consumption and provide higher bandwidth. Moreover, FSO becomes as an alternative or a complementary to the RF communication as it overcomes the problems of the spectrum scarcity and its license access to free frequency band. In this context, many previous attempts have leveraged some these advantages by introducing the FSO into classical systems to be called Mixed Radio-Frequency (RF)/FSO systems [2]–[4]. This new system architecture reduces not only the interference level but also it offers full duplex Gigabit Ethernet throughput and high network security [5]. Although the literature has shown the superiority of the mixed RF/FSO systems over the classical RF systems, they still suffer from the reliability scarcity and power efficient coverage. To overtake this difficulty, previous research attempts have proposed cooperative relaying techniques hybridized with the mixed RF/FSO systems since it improves not only the capacity of the wireless system but also it offers high Quality of Service (QoS). Recently, this new efficient system model has attracted considerable attention in particular using various relaying schemes. The most common used relaying

techniques are Quantize-and-Encode [6], Decode-and-Forward [4] and Amplify-and-Forward [7]. In practice, however, the hardware (source, relays, destination) are susceptible to impairments, e.g., High Power Amplifier (HPA) nonlinearities [8] phase noise [9] and In Phase and Quadrature (IQ) imbalance [10]. Due to its low quality and price, the relay suffers from the nonlinear Power Amplifier (PA) impairment which is caused primarily by the non-linear amplification of the signal that may cause a distortion and a phase rotation of the signal. The most common nonlinear HPA model are Traveling Wave Tube Amplifier (TWTA), Soft Envelope Limiter (SEL) [11] and Ideal Soft Limiter Amplifier (ISLA) [12]. Maletic *et al.* [11] concluded that the SEL has less severe impact on the system performance than the TWTA model. Furthermore, there are few attempts [13] considering mixed RF/FSO system affected by a general model of impairments but they did not specify the type/nature of the hardware impairments. In this work, we propose a mixed RF/FSO system with multiple relays employing Fixed Gain (FG) relaying. Since the channels are subject to time selectivity due to the mobility and Doppler spread, we assume partial relay selection (PRS) based on the outdated Channel State Information (CSI) of the first hop [13]. Besides, we assume that the relays are vulnerable to either SEL or TWTA impairments while the destination suffers from IQ imbalance. The rest of this paper is organized as follows: the system model is presented in Section II. The analysis of the outage probability and the ergodic capacity is provided in Sections III and IV, respectively. Section V discusses the numerical and simulation results while the concluding remarks and the future directions are given in Section VI.

II. SYSTEM MODEL

The system consists of a source (S) communicating with a destination (D) through N parallel relays shown by Fig. 1. For a given transmission, S periodically receives the CSIs ($\gamma_{1(\ell)}$ for $\ell = 1 \dots N$) of the first hop from the N relays and sorts them in an increasing order of magnitude as follows: $\gamma_{1(1)} \leq \gamma_{1(2)} \leq \dots \leq \gamma_{1(N)}$. The perfect scenario is to select the best relay ($m = N$) but this best one is not always available. In this case, S will select the next best available relay. Consequently, the PRS protocol selects the m -th worst or $(N - m)$ -th best relay R_m . Given that the feedback is delayed due to the time selectivity caused by the mobility and Doppler spread, the CSI at the time of selection is different from the CSI at the instant of transmission. In this case, outdated CSI should be assumed

Elyes Balti is with the Wireless Networking and Communications Group, Department of Electrical and Computer Engineering, The University of Texas at Austin, Austin, TX 78712 USA e-mail: ebalti@utexas.edu.

Neji Mensi and Danda B. Rawat are with the Department of Electrical Engineering and Computer Science, Howard University, Washington, DC, 20059 USA e-mail: neji.mensi@bison.howard.edu, danda.rawat@howard.edu.

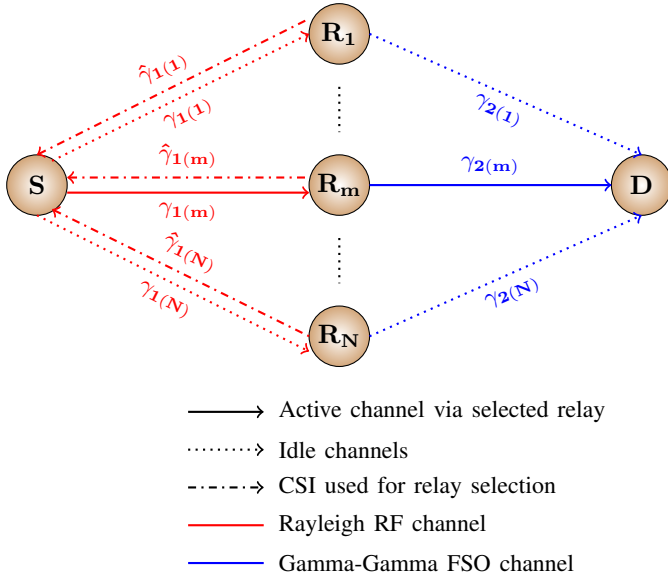


Fig. 1: Mixed RF/FSO system with partial relay selection

instead of perfect CSI estimation. Hence, the instantaneous CSI used for relay selection $\hat{\gamma}_{1(m)}$ and the instantaneous CSI $\gamma_{1(m)}$ used for transmission are correlated with the temporal correlation ρ . The received signal at the m -th relay is given by

$$y_{1(m)} = h_m s + \nu_1 \quad (1)$$

where $s \in \mathbb{C}$ is the information signal, h_m is the RF fading between S and R_m and $\nu_1 \sim \mathcal{CN}(0, \sigma_0^2)$ is the Additive White Gaussian Noise (AWGN).

A. High Power Amplifier nonlinearities at the relays

The PA nonlinearities impairment is introduced to the relays. The amplification of the signal happens in two time slots. In the first slot, the received signal at the relay R_m is amplified by a proper gain G as $\phi_m = G y_{1(m)}$. The gain G can be defined as

$$G = \sqrt{\frac{\sigma^2}{\mathbb{E}[|h_m|^2] P_1 + \sigma_0^2}} \quad (2)$$

where $\mathbb{E}[\cdot]$ is the expectation operator, P_1 is the average transmitted power from S and σ^2 is the mean power of the signal at the output of the relay block. In the second time slot, the signal passes through a nonlinear circuit $\psi_m = f(\phi_m)$. The PA of the relay is assumed to be memoryless. A memoryless PA is characterized by both Amplitude to Amplitude (AM/AM) and Amplitude to Phase (AM/PM) characteristics. The functions AM/AM and AM/PM transform the signal distortion respectively to $A_m(|\phi_m|)$ and $A_p(|\phi_m|)$ and then the output signal of the nonlinear PA circuit is given by

$$\psi_m = A_m(|\phi_m|) e^{j(\text{angle}(\phi_m) + A_p(|\phi_m|))} \quad (3)$$

The characteristic functions of the SEL and TWTA impairments models are respectively given by [3]. From a given saturation level A_{sat} , the relay's PA operates at an input back-off (IBO), which is defined by $\text{IBO} = \frac{A_{\text{sat}}^2}{\sigma^2}$. According to

Bussgang Linearization Theory [8], the output of the nonlinear PA circuit linearly depends on both the linear scale δ of the input signal and a nonlinear distortion d which is uncorrelated with the input signal and follows the circularly complex Gaussian random variable $d \sim \mathcal{CN}(0, \sigma_d^2)$. Then, the AM/AM characteristic $A_m(|\phi_m|)$ can be expressed as follows

$$A_m(|\phi_m|) = \delta |\phi_m| + d. \quad (4)$$

Note that δ and σ_d^2 for SEL and TWTA are given by [3]. Then at the relay R_m , the RF amplified signal is converted to an optical one which is given by [13]

$$r_m = G(1 + \eta \psi_m) \quad (5)$$

where η is the electrical-to-optical conversion coefficient.

B. In Phase and Quadrature Imbalance at the destination

In case of perfect IQ mismatch, the received signal at the destination can be expressed as follows

$$y_{2(m)} = I_m G \eta \psi_m + \nu_2 \quad (6)$$

where I_m is the optical irradiance between the relay R_m and D , η is the optical-to-electrical conversion coefficient, and $\nu_2 \sim \mathcal{CN}(0, \sigma_0^2)$ is the AWGN.

Given that the destination is affected by IQ imbalance, the received signal is given by

$$\hat{y}_{2(m)} = \omega_1 y_{2(m)} + \omega_2 y_{2(m)}^* \quad (7)$$

where $y_{2(m)}^*$ is called the mirror signal introduced by the IQ imbalance at D and the coefficients ω_1 and ω_2 are respectively given by

$$\omega_1 = \frac{1 + \zeta e^{-j\theta}}{2} \quad (8)$$

$$\omega_2 = \frac{1 - \zeta e^{j\theta}}{2} \quad (9)$$

where θ and ζ are respectively the phase and the magnitude imbalance. This impairment is modeled by the Image-Leakage Ratio (ILR), which is given by $\text{ILR} = \left| \frac{\omega_2}{\omega_1} \right|^2$. For an ideal D , $\theta = 0$, $\zeta = 1$, $\omega_1 = 1$, $\omega_2 = 0$, and $\text{ILR} = 0$.

C. Channels Models

Since the RF channels are subject to correlated Rayleigh fading, the Cumulative Distribution Function (CDF) of the instantaneous RF SNR $\gamma_{1(m)}$ is given by [13, Eq. (9)]

$$F_{\gamma_{1(m)}}(x) = 1 - m \binom{N}{m} \sum_{n=0}^{m-1} \binom{m-1}{n} \frac{(-1)^n}{N - m + n + 1} \times \exp\left(-\frac{(N - m + n + 1)x}{((N - m + n)(1 - \rho) + 1)\bar{\gamma}_1}\right). \quad (10)$$

Since the instantaneous SNR $\gamma_{2(m)}$ experiences Gamma-Gamma fading, the Probability Density Function (PDF) is given by

$$f_{\gamma_{2(m)}}(x) = \frac{(\alpha\beta)^{\frac{\alpha+\beta}{2}} x^{\frac{\alpha+\beta}{4}-1}}{2\Gamma(\alpha)\Gamma(\beta)\bar{\gamma}_2^{\frac{\alpha+\beta}{4}}} G_{0,2}^{2,0}\left(\begin{matrix} - \\ \frac{\alpha-\beta}{2}, \frac{\beta-\alpha}{2} \end{matrix} \middle| \alpha\beta\sqrt{\frac{x}{\bar{\gamma}_2}}\right) \quad (11)$$

where $G_{p,q}^{m,n} \left(\begin{matrix} \mathbf{a}_n, \mathbf{a}_p \\ \mathbf{b}_m, \mathbf{b}_q \end{matrix} \middle| \cdot \right)$ is the Meijer-G function, α and β are respectively the small-scale and large-scale of the scattering process in the atmospheric environment. These parameters are given by

$$\alpha = \left(\exp \left[\frac{0.49\sigma_R^2}{(1 + 1.11\sigma_R^{\frac{12}{5}})^{\frac{7}{6}}} \right] - 1 \right)^{-1} \quad (12)$$

$$\beta = \left(\exp \left[\frac{0.51\sigma_R^2}{(1 + 0.69\sigma_R^{\frac{12}{5}})^{\frac{5}{6}}} \right] - 1 \right)^{-1} \quad (13)$$

where σ_R^2 is called Rytov variance which is a metric of the atmospheric turbulence intensity.

D. End-to-end signal-to-noise-plus-distortion ratio (SNDR)

The average SNR of the first hop is given by

$$\bar{\gamma}_1 = \frac{P_1 |h_m|^2}{\sigma_0^2} \quad (14)$$

While the average SNR $\bar{\gamma}_2^{-1}$ of the second hop can be expressed as

$$\bar{\gamma}_2 = \frac{\mathbb{E}[I_m^2]}{\mathbb{E}[I_m]^2} \mu_2 \quad (15)$$

where μ_2 is the average electrical SNR given by

$$\mu_2 = \frac{\eta^2 \mathbb{E}[I_m]^2}{\sigma_0^2}. \quad (16)$$

According to [11, Eq. (16)], the end-to-end SNDR is given by

$$\text{SNDR} = \frac{\gamma_{1(m)} \gamma_{2(m)}}{\text{ILR} \gamma_{1(m)} \gamma_{2(m)} + (1 + \text{ILR})(\mathbb{E}[\gamma_{1(m)}] + \kappa \gamma_{2(m)} + \kappa)} \quad (17)$$

where $\mathbb{E}[\gamma_{1(m)}]$ is given by [13, Eq. (10)] and the term κ is defined as the ratio between the received SNR and the average transmitted SNDR at the relay which is given by

$$\kappa = 1 + \frac{\sigma_d^2}{\delta^2 G^2 \sigma_0^2}. \quad (18)$$

III. OUTAGE PROBABILITY

A. Exact Analysis

The outage probability is defined as the probability that the SNDR falls below a given outage threshold x . It can be written as follows

$$P_{\text{out}}(\text{SNDR}, x) = \mathbb{P}[x \leq \text{SNDR}] = F_{\text{SNDR}}(x) \quad (19)$$

where $F_{\text{SNDR}}(\cdot)$ is the CDF of the SNDR.

Theorem 1. *Under joint effects of HPA nonlinearities and IQ imbalance, the outage probability is given by (20) if $x < \frac{1}{\text{ILR}}$, otherwise, it is equal to 1.*

¹The average SNR $\bar{\gamma}_2$ is defined as $\bar{\gamma}_2 = \eta^2 \mathbb{E}[I_m^2] / \sigma_0^2$, while the average electrical SNR μ_2 is given by $\mu_2 = \eta^2 \mathbb{E}[I_m]^2 / \sigma_0^2$. Therefore, the relation between the average SNR and the average electrical SNR is trivial given that $\frac{\mathbb{E}[I_m^2]}{\mathbb{E}[I_m]^2} = \sigma_{\text{si}}^2 + 1$, where σ_{si}^2 is the scintillation index [14].

$$P_{\text{out}}(\text{SNDR}, x) = 1 - \frac{2^{\alpha+\beta-2}}{\pi \Gamma(\alpha) \Gamma(\beta)} m \binom{N}{m} \sum_{n=0}^{m-1} \frac{(-1)^n}{N - m + n + 1} \binom{m-1}{n} \exp \left(- \frac{(N - m + n + 1) \kappa (1 + \text{ILR}) x}{((N - m + n)(1 - \rho) + 1)(1 + \text{ILR}) \bar{\gamma}_1} \right) G_{0,5}^{5,0} \left(\begin{matrix} - \\ \mathbf{b} \end{matrix} \middle| \frac{(\alpha\beta)^2 (\mathbb{E}[\gamma_{1(m)}] + \kappa)(N - m + n + 1)x}{16((N - m + n)(1 - \rho) + 1)(1 + \text{ILR}) \bar{\gamma}_1 \bar{\gamma}_2} \right) \quad (20)$$

where $\mathbf{b} = [\frac{\alpha}{2}, \frac{\alpha+1}{2}, \frac{\beta}{2}, \frac{\beta+1}{2}, 0]$.

Proof. After transforming the exponential into Meijer-G function and applying the identity [15, Eq. (07.34.21.0013.01)], the outage is derived as (20). \square

B. High SNR Analysis

Using [15, Eq. (07.34.06.0001.01)] to expand the Meijer-G function in (20) at high SNR, the expansion is given by

$$G_{0,5}^{5,0} \left(\begin{matrix} - \\ \mathbf{b} \end{matrix} \middle| z \right) \cong \sum_{k=1}^5 \prod_{j=1, j \neq k}^5 \Gamma(b_j - b_k) z^{b_k} \quad (21)$$

where b_k is the k -th element of the vector \mathbf{b} .

C. Diversity Analysis

Given that the outage performance saturates at high SNR by the floor caused by the hardware impairments, it is trivial to conclude that the diversity gain G_d is equal to zero. For an ideal hardware and after expanding the Meijer-G function at high SNR, it can be shown that the diversity gain is given by

$$G_d = \begin{cases} \min \left(m, \frac{\alpha}{2}, \frac{\beta}{2} \right) & \text{if } \rho = 1 \\ \min \left(1, \frac{\alpha}{2}, \frac{\beta}{2} \right) & \text{otherwise} \end{cases} \quad (22)$$

IV. ERGODIC CAPACITY

A. Exact Analysis

The ergodic capacity, expressed in bits/s/Hz, is defined as the maximum error-free data transferred by the system channel. It can be written as follows

$$\mathcal{I}(\text{SNDR}) = \mathbb{E}[\log(1 + \varpi \text{SNDR})] \quad (23)$$

where $\varpi = e/2\pi$ for intensity modulation and direct detection (IMDD). The capacity can be calculated by deriving the PDF of the SNDR. However, an exact closed-form of Eq. (23) is not tractable due to the presence of mathematical terms related to the hardware impairments. Thereby, the numerical integration can be performed to evaluate the exact capacity.

B. Approximation

In spite of the difficulty to calculate an exact closed-form of the EC, we can derive a simpler expression by referring to the approximation given by [11, Eq. (27)]

$$\mathbb{E} \left[\log \left(1 + \frac{\psi}{\varphi} \right) \right] \cong \log \left(1 + \frac{\mathbb{E}[\psi]}{\mathbb{E}[\varphi]} \right). \quad (24)$$

Although Eq. (24) has no theoretical foundations, it provides with a tight bound on the capacity.

C. Bound I

For high SNR values, the SNDR converges to SNDR^* defined by

$$\lim_{\bar{\gamma}_1, \bar{\gamma}_2 \rightarrow \infty} \text{SNDR} = \frac{1}{\frac{(1+\text{ILR})\xi}{\delta} - 1} = \text{SNDR}^*. \quad (25)$$

Corollary 1. Suppose that $\bar{\gamma}_1$ and $\bar{\gamma}_2$ converge to infinity and the electrical and optical channels are independent, the ergodic capacity converges to a capacity ceiling defined by

$$\mathcal{I}(\text{SNDR}) \leq \log(1 + \varpi \text{SNDR}^*). \quad (26)$$

Proof. Since the SNDR converges to SNDR^* as the average SNRs of the first and second hops largely increase, the Dominated Convergence Theorem allows to move the limit inside the logarithm function. \square

D. Bound II

If the relaying system is linear, i.e, the system is only impaired by IQ imbalance, the SNDR and the average capacity are saturated at the high SNR regime as follows

$$\lim_{\text{IBO} \rightarrow +\infty} \text{SNDR}^* = \lim_{\text{IBO} \rightarrow +\infty} \frac{1}{\frac{(1+\text{ILR})\xi}{\delta} - 1} = \frac{1}{\text{ILR}}. \quad (27)$$

Corollary 2. For linear relaying, the system capacity under IQ imbalance is bounded at high SNR by

$$\mathcal{I}(\text{SNDR}) \leq \log\left(1 + \frac{\varpi}{\text{ILR}}\right). \quad (28)$$

E. Jensen Bound

To further characterize the ergodic capacity, it is possible to derive the expression of the upper bound stated by the following Theorem.

Theorem 2. For asymmetric (Rayleigh/Gamma-Gamma) fading channels, the ergodic capacity under joint effects of HPA nonlinearities and IQ imbalance is bounded by

$$\mathcal{I}(\text{SNDR}) \leq \log\left(1 + \frac{\varpi \mathcal{J}}{\text{ILR} \mathcal{J} + 1}\right) \quad (29)$$

where \mathcal{J} is given by

$$\mathcal{J} = \mathbb{E}\left[\frac{\gamma_1(m)\gamma_2(m)}{(\text{ILR} + (1 + \text{ILR})\kappa)\gamma_2(m) + (1 + \text{ILR})(\mathbb{E}[\gamma_1(m)] + \kappa)}\right] \quad (30)$$

After some mathematical manipulations, \mathcal{J} is given by

$$\begin{aligned} \mathcal{J} = & \frac{m \binom{N}{m} (\alpha\beta)^{\frac{\alpha+\beta}{2}} \left(\frac{\mathbb{E}[\gamma_1(m)] + \kappa}{\kappa}\right)^{\frac{\alpha+\beta}{4}}}{2\pi(1 + \text{ILR})\kappa\Gamma(\alpha)\Gamma(\beta)\bar{\gamma}_2^{\frac{\alpha+\beta}{4}}} \\ & \times \sum_{n=0}^{m-1} \binom{m-1}{n} \frac{(-1)^n ((N-m+n)(1-\rho)+1)\bar{\gamma}_1}{(N-m+n+1)^2} \\ & \times G_{1,5}^{5,1}\left(\lambda_0 \middle| \frac{(\alpha\beta)^2(\mathbb{E}[\gamma_1(m)] + \kappa)}{16\kappa\bar{\gamma}_2}\right) \end{aligned} \quad (31)$$

where $\lambda_1 = \left[\frac{\alpha-\beta}{4}, \frac{\alpha-\beta+2}{4}, \frac{\beta-\alpha}{4}, \frac{\beta-\alpha+2}{4}, -\frac{\alpha+\beta}{4}\right]$ and $\lambda_0 = -\frac{\alpha+\beta}{4}$.

V. NUMERICAL RESULTS

This Section presents the analytical and numerical² results of the outage probability and ergodic capacity obtained from the mathematical expressions derived in the previous Sections. Unless otherwise stated, we assume that the outage threshold ($x = 10$ dB), the temporal correlation ($\rho = 0.9$), the number of relay ($N = 5$), the rank of selected relay ($m = 2$), and the Rytov variance ($\sigma_R^2 = 0.16$). The dependence of the outage on the joint effects of the HPA nonlinearities and IQ imbalance is illustrated by Fig. 2. In Fig. 2a, we observe that the system is vulnerable to the HPA nonlinearities distortion wherein the outage saturates when the IBO, which is the maximum power delivered by the PA, is very low and vice versa. In fact, when the IBO is lower, the PA is unable to provide sufficient power to the relay to amplify the signal which in turn causes signal clipping resulting in information losses and higher outage. In other terms, the PA devices are nonlinear devices and high power amplification may introduce clipping which is translated in frequency domain as spectral regrowth which in turn causes interference between the adjacent subcarriers or aliasing resulting in information losses. The same analysis follows for the effect of the ILR on the outage which is illustrated by Fig. 2b. We observe that the system performance gets much better for low ILR and vice versa. In fact, the ILR measures the severity of the mismatch at the receiver and as long as the mismatch is pronounced, the outage is higher.

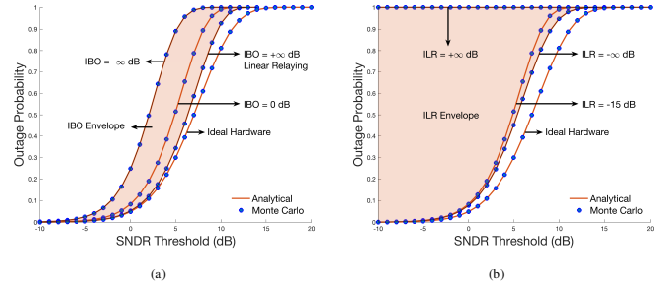


Fig. 2: Performance results of the outage probability at SNR = -10 dB: Fig. 2a illustrates the impacts of the IBO range on the outage while the ILR is fixed at -15 dB. Fig. 2b provides the effects of the ILR range on the outage while the IBO is fixed at 0 dB.

Fig. 3 illustrates the joint effects of HPA nonlinearities and IQ imbalance on the outage and ergodic capacity from different perspectives. In Fig. 3a, we observe that the impact of the hardware impairments is not significant at low SNR, however, this impact becomes remarkable at high SNR wherein the distortion creates an irreducible outage floor. Besides, we note that the introduction of the wireless optical signaling and multiple relays decreases the outage much lower than the conventional RF relaying systems [11] at low SNR. At high SNR, even though both systems are saturated by the outage floor, the proposed system achieves better outage due to the higher diversity order compared to the conventional RF system. The

²For all cases, 10^6 realizations of the random variables were generated to perform the Monte Carlo simulation in MATLAB.

same conclusion can be drawn from Fig. 3b wherein the capacity is saturated at high SNR by a ceiling created by the hardware impairments. We further note that the TWTA introduces more severe deterioration to the system compared to SEL and this result has been confirmed by related works.

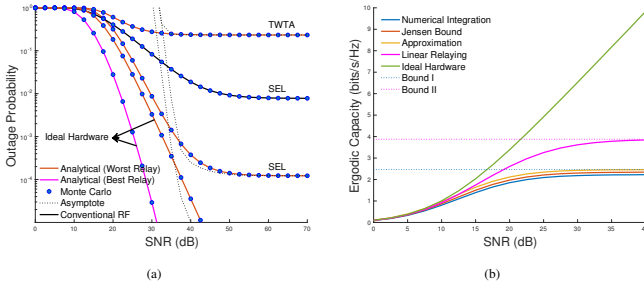


Fig. 3: Performance results: Fig. 3a illustrates a comparison between the SEL and TWTA and their effects on the outage. Fig. 3b presents the impacts of the HPA nonlinearities and IQ imbalance on the spectral efficiency.

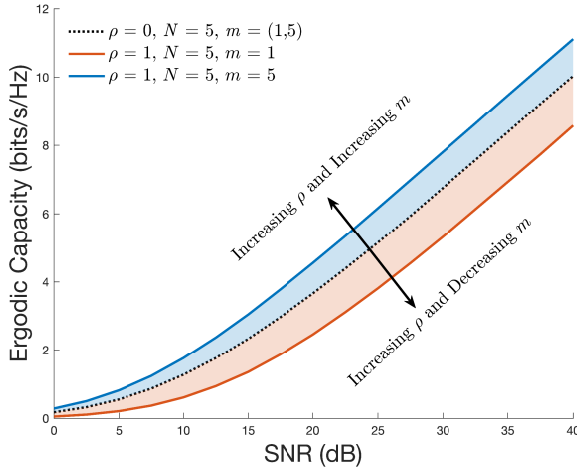


Fig. 4: Performance results: Impacts of the temporal correlation and the rank of the selected relay on the spectral efficiency.

Fig. 4 provides the dependence of the temporal correlation and the rank of the selected relay on the ergodic capacity. Given that the CSI are sorted in increasing order, then the performance improves with the rank of the selected relay. However, this improvement is achieved only when the CSIs are completely correlated ($\rho \cong 1$), i.e., the CSIs at the moments of relay selection and transmission are roughly the same. In other terms, the channels are slowly varying in time. Inversely, if the channels are uncorrelated ($\rho \cong 0$), i.e., the channels are rapidly varying in time, the source does not have any knowledge about the channels conditions and hence the rank does not reflect the best relay selection, i.e., the higher the rank is, the worse the performances are.

VI. CONCLUSION

In this work, we provided the analysis of various models of impairments and their effects on the system performance. We introduced the SEL and TWTA as HPA nonlinearities affecting the relays and we assume that the destination is impaired by

IQ imbalance. We investigated the effects of these hardware imperfections on the outage and capacity and we concluded that the system performs better as the IBO increases and the ILR decreases. Moreover, it turned out that the TWTA has more severe impact on the system performance than the SEL model. Furthermore, even though the performance deteriorates under the effects of the imperfections, we noted that the introduction of the FSO technique and multiple relays makes the mixed RF/FSO system more resilient to the hardware impairments than the conventional RF relaying systems. Besides, we illustrated the performance degradation by the hardware impairments as a form of irreducible outage floor as well as the capacity ceiling at high SNR. Finally, we investigated the impact of the temporal CSI correlation and we concluded that the performance improvement is conditioned upon the channels correlation.

REFERENCES

- [1] M. A. Khalighi and M. Uysal, "Survey on Free Space Optical Communication: A Communication Theory Perspective," *IEEE Communications Surveys Tutorials*, vol. 16, no. 4, pp. 2231–2258, Fourthquarter 2014.
- [2] E. Soleimani-Nasab and M. Uysal, "Generalized performance analysis of mixed rf/fso cooperative systems," *IEEE Transactions on Wireless Communications*, vol. 15, no. 1, pp. 714–727, 2016.
- [3] E. Balti and B. K. Johnson, "On the joint effects of hpa nonlinearities and iq imbalance on mixed rf/fso cooperative systems," 2020.
- [4] E. Balti and B. K. Johnson, "Tractable approach to mmwaves cellular analysis with fso backhauling under feedback delay and hardware limitations," *IEEE Transactions on Wireless Communications*, vol. 19, no. 1, pp. 410–422, 2020.
- [5] E. Balti and N. Mensi, "Zero-forcing max-power beamforming for hybrid mmwave full-duplex mimo systems," in *2020 4th International Conference on Advanced Systems and Emergent Technologies (IC_ASET)*, 2020, pp. 344–349.
- [6] K. Kumar and D. K. Borah, "Quantize and encode relaying through FSO and hybrid FSO/RF links," *IEEE Transactions on Vehicular Technology*, vol. 64, no. 6, pp. 2361–2374, June 2015.
- [7] N. Mensi, D. B. Rawat, and E. Balti, "PLS for V2I communications using friendly jammer and double kappa-mu shadowed fading," in *2021 IEEE International Conference on Communications (ICC): Wireless Communications Symposium (IEEE ICC'21 - WC Symposium)*, Montreal, Canada, Jun. 2021.
- [8] D. Dardari, V. Tralli, and A. Vaccari, "A theoretical characterization of nonlinear distortion effects in OFDM systems," *IEEE Transactions on Communications*, vol. 48, no. 10, pp. 1755–1764, Oct 2000.
- [9] T. Riihonen, S. Werner, F. Gregorio, R. Wichman, and J. Hamalainen, "BEP analysis of OFDM relay links with nonlinear power amplifiers," in *2010 IEEE Wireless Communication and Networking Conference*, April 2010, pp. 1–6.
- [10] J. Qi, S. Aissa, and M. S. Alouini, "Analysis and compensation of I/Q imbalance in amplify-and-forward cooperative systems," in *2012 IEEE Wireless Communications and Networking Conference (WCNC)*, April 2012, pp. 215–220.
- [11] N. Maletic, M. Cabarkapa, and N. Neskovic, "Performance of fixed-gain amplify-and-forward nonlinear relaying with hardware impairments," *International Journal of Communication Systems*, pp. n/a–n/a, 2015.
- [12] C. Zhang, P. Ren, J. Peng, G. Wei, Q. Du, and Y. Wang, "Optimal Relay Power Allocation for Amplify-and-Forward Relay Networks with Non-linear Power Amplifiers," *ArXiv e-prints*, Apr. 2011.
- [13] M. I. Petkovic, A. M. Cvetkovic, G. T. Djordjevic, and G. K. Karagiannidis, "Partial relay selection with outdated channel state estimation in mixed RF/FSO systems," *Journal of Lightwave Technology*, vol. 33, no. 13, pp. 2860–2867, July 2015.
- [14] M. Niu, J. Cheng, and J. F. Holzman, "Error rate performance comparison of coherent and subcarrier intensity modulated optical wireless communications," *J. Opt. Commun. Netw.*, vol. 5, no. 6, pp. 554–564, Jun 2013.
- [15] "The wolfram functions site." [Online]. Available: <http://functions.wolfram.com>